Synthetic, Structural, and Solution Thermochemical Studies in the Dimethylbis(phosphine)platinum(II) System. Dichotomy between Structural and Thermodynamic Trends

Christopher M. Haar and Steven P. Nolan*

Department of Chemistry, University of New Orleans, New Orleans, Louisiana 70148

William J. Marshall and Kenneth G. Moloy

Central Research and Development, E. I. du Pont de Nemours & Co., Inc., Experimental Station, P.O. Box 80328, Wilmington, Delaware 19880-0328

Alfred Prock and Warren P. Giering

Department of Chemistry, Metcalf Science and Engineering Center, Boston University, Boston, Massachusetts 02215

Received August 17, 1998

Reaction enthalpies of the complex (COD)$PtMe_2$ (COD = η^4-1,5-cyclooctadiene) with an extensive series of unidentate phosphines have been measured by solution calorimetry. The molecular structures of *cis*-P_2PtMe_2 for P = PEt_3, PMe_2Ph, P(pyrrolyl)$_3$, and PCy_3 have been determined by single-crystal X-ray diffraction. The relative stabilities of the resulting P_2-$PtMe_2$ complexes are strongly influenced by the size (cone angle) of the incoming phosphine, with larger cone angles resulting in less thermodynamically stable complexes. Crystallographic and ^{31}P NMR data, however, do not reflect the enthalpic stability scale and are more closely correlated to the electronic (χ) character of the phosphine ligands. The strength of the Pt−P interaction, as determined from these structural data, is greatest for phosphines with electron-withdrawing substituents, regardless of phosphine size or reaction enthalpy.

Introduction

The intelligent design of any chemical synthesis involves an understanding of the factors influencing the stability of the target compound. It has long been recognized that the nature of the coordinated phosphine(s) can exert a powerful influence on the structural and catalytic chemistry of transition-metal complexes.[1−3] Owing to platinum's well-developed reaction chemistry, synthetic routes to σ-bonded organoplatinum(II) complexes are numerous.[4] In particular, complexes of the type (COD)PtRX (COD = η^4-1,5-cyclooctadiene; R, X = alkyl, aryl, halide) are known for many combinations of R and X (e.g., **1**). The lability of the COD−Pt interaction renders these compounds convenient sources of organoplatinum fragments for coordination to Lewis bases such as phosphines, according to eq 1. In an effort to better understand the factors which influence the stability of bis(phosphine)platinum(II) species, a thermochemical study of the reaction in eq 1 was undertaken for a series of unidentate tertiary phosphines (**2**) of varying steric and electronic character. The enthalpic data are discussed in terms of both steric and electronic properties of the incoming phosphines and provide an interesting contrast to NMR spectroscopic and X-ray structural data for this series of complexes.

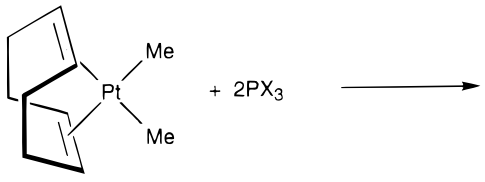

1 **2**

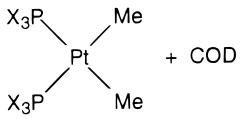

3 (1)

Results and Discussion

As determined by ^1H and ^{31}P NMR spectroscopy, the reaction illustrated by eq 1 is notably fast, clean, and quantitative for a wide variety of tertiary phosphines.

(1) Collman, J. P.; Hegedus, L. S.; Norton, J. R.; Finke, R. G. *Principles and Applications of Organotransition Metal Chemistry*; University Science Books: Mill Valley, CA, 1987.
(2) Parshall, G. W.; Ittel, S. *Homogeneous Catalysis*; Wiley: New York, 1992.
(3) Pignolet, L. H. In *Homogeneous Catalysis with Metal Phosphine Complexes*; Pignolet, L. H., Ed.; Plenum: New York, 1983.
(4) See for example: Anderson, G. K. In *Comprehensive Organometallic Chemistry II*; Abel, E. W., Stone, F. G. A., Wilkinson, G., Eds.; Pergamon: Oxford, U.K., 1995; Vol. 9, pp 431−531.

10.1021/om9807001 CCC: $18.00
Publication on Web 01/16/1999

Table 1. Enthalpies of Substitution (kcal/mol) and NMR Data for the Reaction

$$(COD)PtMe_2(soln) + 2PX_3(soln) \xrightarrow[30\ °C]{CH_2Cl_2} (X_3P)_2PtMe_2(soln) + COD(soln)$$

entry no.	complex	PX_3	$-\Delta H_{rxn}$ (kcal/mol)[a]	$\delta(^{31}P)$ (ppm)[b]	J_{PtP} (Hz)[b]	$\delta(^1H(CH_3))$ (ppm)[b]	J_{PtCH_3} (Hz)[b]
1	**3a**	PMe_3	34.3(0.2)	−23.1	1761	0.30	66
2	**3a**	PEt_3	32.9(0.3)	9.3	1843	0.28	66
3	**3b**	PMe_2Ph	32.0(0.3)	−10.4	1826	0.43	68
4	**3d**	$PMePh_2$	29.0(0.2)	7.6	1854	0.31	68
5	**3e**	P^iBu_3	25.4(0.3)	3.2	1852	0.19	68
6	**3f**	$P(p\text{-}MeC_6H_4)_3$	24.3(0.2)	26.3	1917	0.28	69
7	**3g**	$P(p\text{-}MeOC_6H_4)_3$	23.4(0.2)	24.9	1933	0.29	69
8	**3h**	$P(p\text{-}ClC_6H_4)_3$	23.2(0.1)	27.1	1876	0.37	70
9	**3i**	$P(p\text{-}FC_6H_4)_3$	23.0(0.2)	26.7	1888	0.36	69
10	**3j**	$PPh_2(pyrl)$	22.6(0.3)	69.4	2048	0.54	66
11	**3k**	PPh_3	22.6(0.2)	27.7	1900	0.34	69
12	**3l**	$P(p\text{-}CF_3C_6H_4)_3$	21.5(0.3)	29.0	1850	0.46	70
13	**3m**	P^iPr_3	20.7(0.2)	32.7	1859	0.32	67
14	**3n**	$P(pyrl)_3$	20.4(0.2)	96.6	2506	0.69	70
15	**3o**	$PPh(pyrl)_2$	20.1(0.2)	86.5	2245	0.66	70
16	**3p**	PCy_3	19.2(0.3)	20.1	1828	0.29	67

[a] Enthalpy values are reported with 95% confidence limits. [b] NMR data were recorded in CD_2Cl_2 at 25 °C.

Of 17 phosphines examined, only P^tBu_3 failed to react, presumably due to the steric bulk of this ligand; after 2 days at 30 °C, only a small amount of substitution was apparent by NMR spectroscopy. In all cases, exclusively *cis*-P_2PtMe_2 was formed. Reaction enthalpies, as well as structural data determined by ^{31}P NMR and X-ray crystallography, can be interpreted in terms of the classical steric (θ) and electronic (χ) parameters introduced by Tolman[5] and revised by Giering and others.[6−8] This simple two-parameter model, however, fails to provide a global description of all the observed phenomena in this system. Instead, the most consistent correlations occur primarily among subsets or families of ligands, while correlations between thermochemical and structural measurements illustrate that these properties are not always coupled in a straightforward manner.

Thermochemical Measurements. Measured enthalpies of reaction span a range of 15 kcal/mol (Table 1) and clearly establish that small-θ phosphines give the most stable complexes in the P_2PtMe_2 system. The large and positive slope of the PR_3 line in Figure 1 (for trialkylphosphines $\chi \propto -\theta$[9]) indicates that the reaction enthalpies display a strong, inverse dependence on the cone angle of the incoming ligand. Such an observation is intuitively satisfying, given that phosphine substitution occurs at mutually *cis* positions on platinum. Less obvious, perhaps, is the observation that an isosteric[5,10] series of aryl- and pyrrolylphosphines yield reaction enthalpies which span a mere 4 kcal/mol range for $14.8 < \chi < 41.4$.[7]

A small but significant χ effect is evidenced by the nonzero slope of the line for $P(p\text{-}XC_6H_4)_3$ and $PPh_{3-x}(pyrl)_x$ in Figure 1. Not surprisingly, the slope is

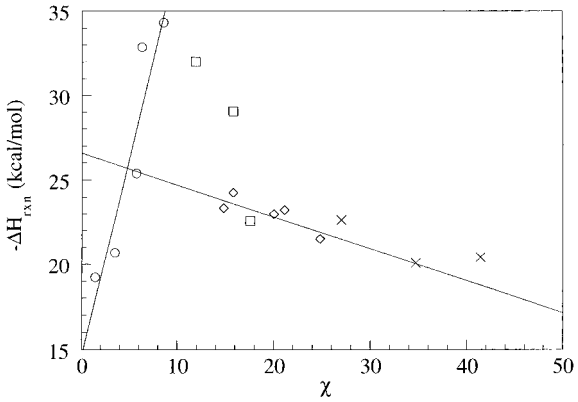

Figure 1. Enthalpy of reaction vs phosphine electronic parameter for $(COD)PtMe_2 + 2PX_3$: (circles) $P(alkyl)_3$ (slope 2.34, $R = 0.932$); (squares) $PMe_{3-x}Ph_x$; (diamonds) $P(p\text{-}XC_6H_4)_3$ (slope −0.189, $R = 0.769$); (crosses) $PPh_{3-x}(pyrl)_x$.

negative, which indicates that $-\Delta H$ becomes larger as the phosphines become better electron donors. Previous thermochemical measurements have shown that, in the absence of steric effects, relative enthalpic stability is enhanced for electron-rich ligands if the incoming phosphine interacts through the metal center with an electron-accepting ligand, e.g., CO in $Rh(CO)(Cl)(PR_3)_2$[11,12] and $(PR_3)_2Fe(CO)_3$.[13−17] Conversely, in electron-rich metal-centered systems such as the ^{R}[PNP]Rh(L) system (^{R}[PNP] = $(R_2PCH_2SiMe_2)_2N^-$; R = i-Pr, Ph),[18] in which the rhodium center is quite electron rich due to both phosphine and amide donor properties, stability is enhanced by electron-poor/π-accepting ligands such as CO or pyrrolyl-substituted phosphines. The clearly

(5) Tolman, C. A. *Chem. Rev.* **1977**, *77*, 313−348.
(6) Fernandez, A.; Reyes, C.; Wilson, M. R.; Woska, D. C.; Prock, A.; Giering, W. P. *Organometallics* **1997**, *16*, 342−348 and references therein.
(7) Fernandez, A. L.; Lee, T. Y.; Reyes, C.; Prock, A.; Giering, W. P. Submitted for publication.
(8) Fernandez, A.; Reyes, C.; Lee, T.-Y.; Prock, A.; Giering, W. P. Submitted for publication.
(9) Bartholomew, J.; Fernandez, A. L.; Lorsbach, B. A.; Wilson, M. R.; Prock, A.; Giering, W. P. *Organometallics* **1996**, *15*, 295−301.
(10) Moloy, K. G.; Petersen, J. L. *J. Am. Chem. Soc.* **1995**, *117*, 7696−7710.
(11) Huang, A.; Marcone, J. E.; Mason, K. L.; Marshall, W. J.; Moloy, K. G.; Serron, S.; Nolan, S. P. *Organometallics* **1997**, *16*, 3377−3380.
(12) Serron, S. A.; Nolan, S. P.; Moloy, K. G. *Organometallics* **1996**, *15*, 4301−4306.
(13) Serron, S. A.; Nolan, S. P. *Inorg. Chim. Acta* **1996**, *252*, 107−113.
(14) Li, C.; Stevens, E. D.; Nolan, S. P. *Organometallics* **1995**, *14*, 3791−3797.
(15) Li, C.; Nolan, S. P. *Organometallics* **1995**, *14*, 1327−1332.
(16) Luo, L.; Nolan, S. P. *Inorg. Chem.* **1993**, *32*, 2410−2415.
(17) Luo, L.; Nolan, S. P. *Organometallics* **1992**, *11*, 3483−3486.
(18) Huang, J.; Haar, C. M.; Nolan, S. P.; Marshall, W. J.; Moloy, K. G. *J. Am. Chem. Soc.* **1998**, *120*, 7806−7815 and references therein.

inverse, albeit weak, correlation of the reaction enthalpy to χ in the present case is similar to the results observed in the (acac)Rh(CO)(PR_3) system (acac = 2,4-pentanedionato).[19] This suggests that both (acac)Rh(CO) and $PtMe_2$ fragments lie in some intermediate domain, perhaps one in which the synergistic bonding patterns observed in the above-mentioned systems do not obtain.

Regression analysis of the thermochemical data does not require the introduction of the aryl (E_{ar}, which accounts for the disparate trends observed in alkyl- and arylphosphine physicochemical properties[20]) or pyrrolyl (π_{pyrl}, similar to E_{ar}, but related to π-acceptor character in *N*-pyrrolylphosphines[8]) electronic parameters in order to achieve a satisfactory fit. The point of intersection of the P(*p*-XC_6H_4)$_3$ and PR_3 lines in Figure 1 is close to $\chi = 5$, which indicates that E_{ar} is not important.[9] This is confirmed by the regression analyses: when the E_{ar} parameter is included in the analysis of P(*p*-XC_6H_4)$_3$ and PR_3, no improvement is seen in the correlation, while the E_{ar} coefficient has a very large standard error. The π effect for the pyrrolyl ligands is equally problematic. The inclusion of the π_{pyrl} parameter also does not improve the correlation, and the standard error of the π_{pyrl} coefficient, too, is large. Statistically and graphically, therefore, it appears that both aryl and pyrrolyl effects are either small or entirely absent, and the thermodynamic data for the 16 ligands can be analyzed in terms of the two-parameter model shown in eq 2,

$$\Delta H_{rxn}\ (\text{kcal/mol}) = (0.35 \pm 0.03)\theta + (0.19 \pm 0.03)\chi - (77.8 \pm 3.6) \quad r^2 = 0.946 \quad (2)$$

which corresponds to steric and electronic contributions of 71% and 29%, respectively. Thus, both large θ (larger) and high χ (less basic) ligands destabilize $(PX_3)_2PtMe_2$, although steric effects seem to play a more significant role.

NMR Spectroscopy. Included in Table 1 are the experimentally determined ^{31}P and ^{1}H NMR data for all compounds investigated in the present study.[21] These data were typical of square-planar platinum with a *cis* arrangement of phosphine and methyl ligands. The Pt−CH_3 resonances appear in ^{1}H spectra as phosphorus-coupled multiplets with ^{195}Pt satellites ($^{2}J_{PtH}$ = 66−70 Hz), while ^{31}P resonances are singlets with ^{195}Pt satellites ($^{1}J_{PtP}$, = 1761−2506 Hz, within the typical range for *cis*-bis(phosphine) species). It is interesting to note that while ^{31}P chemical shifts and $^{1}J_{PtP}$ were highly dependent on the identity of the phosphine, virtually none of this information is transferred across platinum to the methyl groups: the Pt−CH_3 signals display only a weak downfield shift on going to higher χ phosphines, while $^{2}J_{PtH}$ was basically insensitive to variation of the phosphine ligand.

In contrast to thermochemical data, the ^{31}P NMR parameters are much more sensitive to the electronic properties of the phosphine ligands. Graphical analysis of $^{31}P\{^{1}H\}$ chemical shifts clearly divides the set of 16 ligands into 4 distinct families (Figure 2). The slope of the P(*p*-XC_6H_4)$_3$ line indicates a small χ effect, with downfield shifts for the more electron-poor phosphines. The slope of the PR_3 line differs greatly from that of the P(*p*-XC_6H_4)$_3$ line, thereby indicating a severe steric effect, in agreement with the analysis of $-\Delta H$. It is unclear whether the PCy_3 point is anomalously low (correlation of the PR_3 data is greatly improved if the PCy_3 datum is neglected) or indicative of a steric threshold (θ_{st}, the cone angle above which steric effects change[9]). There appears to be no significant aryl effect, since the lines for P(*p*-XC_6H_4)$_3$ and PR_3 intersect near $\chi = 5$, and for the $PMe_{3-x}Ph_x$ series the chemical shift trend is essentially that expected on the basis of sterics alone. The large and systematic deviation of the data for $PPh_{3-x}(pyrl)_x$ indicates the significant influence of the pyrrolyl substituent, consistent with either a π-effect or simple inductive effects arising from the electronegativity of the pyrrolyl group. (Of course, these phenomena may be interrelated.)

Platinum−phosphorus coupling constants display the same general trends as phosphorus chemical shifts, and again, the ligands can be divided into four distinct families (Figure 3). The χ effect is even more evident across the P(*p*-XC_6H_4)$_3$ series, with the better electron donors displaying an increased coupling constant. In the

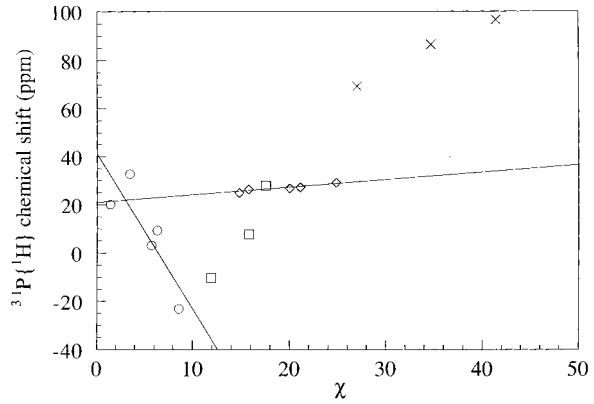

Figure 2. ^{31}P chemical shift vs phosphine electronic parameter (χ) in $(PX_3)_2PtMe_2$: (circles) P(alkyl)$_3$ (slope −6.45, R = 0.846); (squares) $PMe_{3-x}Ph_x$; (diamonds) P(*p*-XC_6H_4)$_3$ (slope 0.312, R = 0.843); (crosses) $PPh_{3-x}(pyrl)_x$.

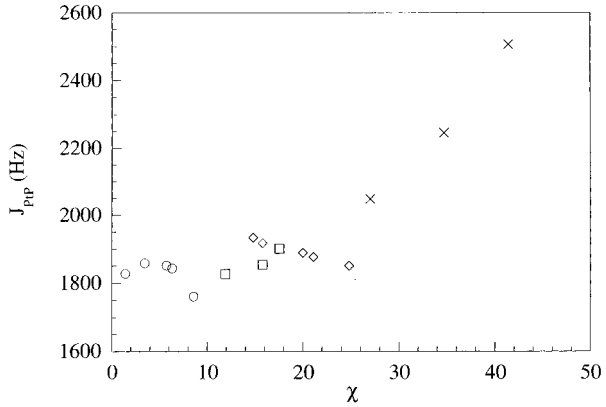

Figure 3. Platinum−phosphorus coupling constants vs phosphine electronic parameter (χ) in $(PX_3)_2PtMe_2$: (circles) P(alkyl)$_3$; (squares) $PMe_{3-x}Ph_x$; (diamonds) P(*p*-XC_6H_4)$_3$; (crosses) $PPh_{3-x}(pyrl)_x$.

(19) Serron, S.; Huang, J.; Nolan, S. P. *Organometallics* **1998**, *17*, 534−539.

(20) Wilson, M. R.; Woska, D. C.; Prock, A.; Giering, W. P. *Organometallics* **1993**, *12*, 1742−1752.

(21) Spectroscopic data for many of these complexes have previously been reported, but to ensure the greatest consistency during data analysis, all NMR data in Table 1 were acquired from NMR titrations performed prerequisite to the calorimetric measurements (see Experimental Section). The data from the present study compare favorably to the literature values.

Table 2. Crystallographic Data for the Complexes P_2PtMe_2

	3b	**3c**	**3n**	**3p**·CH_2Cl_2
formula	$C_{14}H_{36}P_2Pt$	$C_{18}H_{28}P_2Pt$	$C_{26}H_{30}N_6P_2Pt$	$C_{39}H_{74}Cl_2P_2Pt$
fw	461.48	501.46	683.61	870.97
color	light amber	faint amber	light amber	colorless
space group	$P2_1/n$ (No. 14)	$C2/c$ (No. 15)	$P2_1/c$ (No. 14)	$Pbca$ (No. 61)
a, Å	8.148(2)	17.098(4)	9.252(1)	17.702(1)
b, Å	17.543(5)	13.949(3)	15.607(4)	18.102(1)
c, Å	12.780(5)	17.040(3)	18.638(3)	25.137(1)
β, deg	93.67(3)	108.73(2)	95.04(1)	
Z	4	8	4	8
μ(Mo), cm^{-1}	79.34	75.24	54.31	37.56
R^a	0.029	0.040	0.036	0.039
$R_w{}^a$	0.025	0.030	0.033	0.041
no. of refined params	154	190	316	451
no. of data collected	8276	9194	6563	83 404
no. of unique data, $I > 3\sigma(I)$	2963	2276	3940	5589
R_{merge} (%)	2.6	3.2	1.5	2.5

[a] $R = \sum(||F_o| - |F_c||)/\sum|F_o|$; $R_w = \sum w(|F_o| - |F_c|)^2/\sum w|F_o|$.

Table 3. Pertinent Metrical Parameters in P_2PtMe_2 (P = PEt_3, $PPhMe_2$, PPh_2Me, $P(pyrl)_3$, PCy_3)

	PEt_3	PMe_2Ph	$PMePh_2$[a]	$P(pyrl)_3$	PCy_3
			Bond Distances (Å)		
Pt−P(1)	2.290(1)	2.284(3)	2.285(2)	2.249(1)	2.344(1)
Pt−P(2)	2.295(2)	2.285(3)	2.284(2)	2.252(2)	2.330(1)
Pt−C(1)	2.102(5)	2.096(11)	2.122(6)	2.086(7)	2.132(6)
Pt−C(2)	2.099(5)	2.075(11)	2.119(5)	2.123(6)	2.126(5)
			Bond Angles (deg)		
P(1)−Pt−P(2)	100.03(5)	95.0(1)	97.75(6)	97.36(7)	108.60(5)
P(1)−Pt−C(1)	86.1(2)	90.2(3)	93.0(2)	89.8(2)	85.8(2)
P(1)−Pt−C(2)	169.1(2)	175.1(3)	173.7(2)	173.5(2)	164.7(2)
P(2)−Pt−C(1)	173.7(2)	174.4(3)	168.9(2)	172.7(2)	165.1(2)
P(2)−Pt−C(2)	90.7(2)	89.7(3)	87.2(2)	89.1(2)	86.6(2)
C(1)−Pt−C(2)	83.1(2)	85.1(4)	81.9(2)	83.7(3)	79.1(2)

[a] From ref 24.

PR_3 series, a steric threshold may exist at $\chi = 5$, corresponding to $\theta_{st} = 145°$, consistent with the analysis of Romeo and Alibrandi.[22] Considered without a steric threshold, however, the line for PR_3 is essentially parallel (although with much larger standard error for the slope) to that for $P(p\text{-}XC_6H_4)_3$, which would imply no steric component and a significant aryl effect.[9] The effect of pyrrolyl substituents is clear from the large and systematic variations of $PPh_{3-x}(pyrl)_x$ data from the $P(p\text{-}XC_6H_4)_3$ line, though again it is unclear if these results arise from increased Pt−P π interactions or from the increased s-character of the $PPh_{3-x}(pyrl)_x$ σ-orbital.[23]

X-ray Structural Studies. In an effort to clarify the relationship between phosphine ligand steric and electronic properties and the thermochemical and spectroscopic data, single-crystal X-ray diffraction analyses of the PEt_3 (**3b**), PMe_2Ph (**3c**), $P(pyrl)_3$ (**3n**), and PCy_3 (**3p**) adducts were performed (Table 2). Selected metrical parameters for these complexes and the $PMePh_2$ adduct **3d**[24] are given in Table 3. In their gross structural features, all five complexes are typical for square-planar Pt(II). Although deviations from this idealized structure are evident in each complex, no unusual interatomic distances were observed.[25]

Average Pt−P bond lengths range from 2.250 Å in **3n** to 2.337 Å in **3p**. Interestingly, the Pt−P(1) and Pt−P(2) distances are significantly different in **3p** (2.344(1) and 2.330(1) Å, respectively), whereas in the remaining complexes the two distances are essentially indistinguishable. The significantly longer bonds in **3p** can be explained by the extreme bulk of the PCy_3 ligands; the remaining Pt−P distances, however, cannot be rationalized entirely on steric grounds. Bond lengths do increase with θ, but **3n** displays an anomalously short Pt−P contact. Conversely, Pt−P distances decrease with increasing χ, although in this case the exception is **3p**, in which this contact is anomalously long. The P(1)−Pt−P(2) angles display similar trends: increasing from 95.0(1)° in **3c** to 108.60(5)° in **3p**, the angle generally opens up with θ, but the angle in **3n** is somewhat smaller than predicted on the basis of the other complexes. As might be expected, no clear relationship between ∠P(1)−Pt−P(2) and χ appears to exist, and either **3n** or **3p** could be considered deviant.

Average $Pt-C_{methyl}$ distances span a range from 2.086 Å (**3c**) to 2.129 Å (**3p**) and appear somewhat less sensitive to the identity of the phosphine ligand than the Pt−P distances. In general, these distances increase with θ and decrease with χ, although no obvious trends are apparent. In contrast to the Pt−P distances, the Pt−C(1) and Pt−C(2) distances are significantly different in **3n** (2.086(7) and 2.123(6) Å, respectively) and indistinguishable in the other complexes (including **3p**). Complementary to the observations for the phosphorus ligands, ∠C(1)−Pt−C(2) decreases as θ, and thus ∠P(1)−Pt−P(2), increases, and the angle in **3n** is somewhat larger than expected. Again, no clear correlation between χ and ∠C(1)−Pt−C(2) is evident.

Correlations between Structural and Thermodynamic Data. The most remarkable relationship between structural and thermodynamic data is that reaction enthalpies are smallest in the complexes with the shortest Pt−P bond lengths, as is apparent in Figure 4. The exception is the PCy_3 adduct, in which steric contributions surely destabilize **3p** relative to the other complexes. Similarly, although bond length/strength conclusions based on J_{MP} can be misleading,[23] there is a general tendency toward lower reaction enthalpies in complexes with higher J_{PtP} values. The classic rule of "shorter bond equals stronger bond" may *appear* to have been violated, but it cannot be overemphasized that thermochemical measurements such as described here can only determine the total energy difference between

(22) Romeo, R.; Alibrandi, G. *Inorg. Chem.* **1997**, *36*, 4822−4830.
(23) Alyea, E. C.; Song, S. *Inorg. Chem.* **1995**, *34*, 3864−3873.
(24) Wisner, J. M.; Bartczak, T. J.; Ibers, J. A. *Organometallics* **1986**, *5*, 2044−2050.
(25) See, for example, ref 23 and references therein.

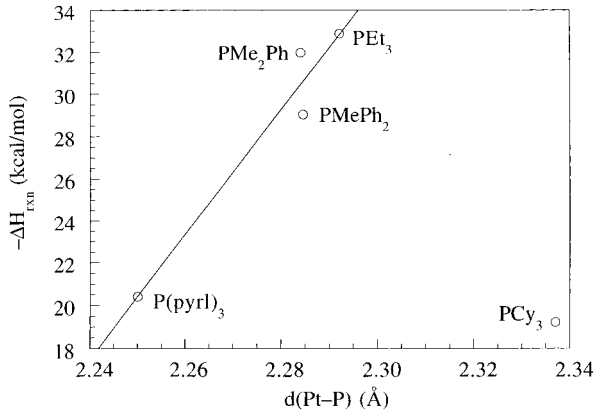

Figure 4. Reaction enthalpy as a function of Pt−P bond length in $(PX_3)_2PtMe_2$ (slope 2.95, $R = 0.975$).

states. Energy terms due to distortions in the Pt coordination environment and internal ligand structure, i.e., reorganization energies,[18,26] may induce a net destabilizing effect regardless of the intrinsic Pt−P bond strength.

Experimental Section

General Considerations. All manipulations were performed under inert atmospheres of argon or nitrogen using standard high-vacuum or Schlenk-line techniques, or in a glovebox containing less than 1 ppm of oxygen and water. Solvents, including deuterated solvents for NMR analysis, were dried by standard methods[27] and distilled under nitrogen or vacuum-transferred before use. NMR spectra were recorded using Varian Gemini 300 MHz or Varian Unity 400 MHz spectrometers. Elemental analyses were performed by Desert Analytics. Only materials of high purity as indicated by NMR spectroscopy were used in the calorimetric experiments. Calorimetric measurements were performed using a Calvet calorimeter (Setaram C-80) which was periodically calibrated using the TRIS reaction[28] or the enthalpy of solution of KCl in water.[29] This calorimeter has been previously described,[30,31] and typical procedures are described below. Experimental enthalpy data are reported with 95% confidence limits.

Complexes **3a**−**h**,**k**,**m**,**p** have been reported previously.[22] The ligands PPh_2(pyrrolyl), PPh(pyrrolyl)$_2$, and P(pyrrolyl)$_3$[10] were synthesized according to literature procedures, as was (COD)$PtMe_2$.[32] Triphenylphosphine and P^{i}Bu$_3$ (Aldrich) and $PMePh_2$, PMe_2Ph, PMe_3, PEt_3, P^{i}Pr$_3$, PCy_3, and P(*p*-XC_6H_4)$_3$ (X = F, Cl, Me, OMe, CF_3) (Strem) were used as received.

NMR Titrations. Prior to every set of calorimetric experiments involving a new ligand, a precisely measured amount (±0.1 mg) of (COD)$PtMe_2$ was placed in an NMR tube along with CD_2Cl_2 and >1.2 equiv of ligand. Both ^{1}H and ^{31}P NMR spectra were measured within 1 h of mixing; both indicated that the reactions were clean and quantitative. These conditions are necessary for accurate and meaningful calorimetric results and were satisfied for all reactions investigated.

Solution Calorimetry. In a representative experimental trial, the mixing vessels of the Setaram C-80 were cleaned, dried in an oven maintained at 120 °C, and then taken into the glovebox. A sample of (COD)$PtMe_2$ (19.4 mg, 58.2 μmol) was massed into the lower vessel, which was closed and sealed with 1.5 mL of mercury. A solution of PPh_3 (37.8 mg, 144 μmol) in CH_2Cl_2 (4 mL) was added, and the remainder of the cell was assembled, removed from the glovebox, and inserted into the calorimeter. The reference vessel was loaded in an identical fashion, with the exception that no platinum complex was added to the lower vessel. After the calorimeter had reached thermal equilibrium at 30.0 °C (ca. 2 h), it was inverted, thereby allowing the reactants to mix. The reaction was considered complete after the calorimeter had once again reached thermal equilibrium (ca. 2 h). Control reactions with Hg and phosphine show no reaction. The enthalpy of ligand substitution (−22.6 ± 0.2 kcal/mol) listed in Table 1 represents the average of at least three individual calorimetric determinations with all species in solution. The enthalpy of solution of (COD)$PtMe_2$ (+5.8 ± 0.1 kcal/mol) in neat CH_2Cl_2 was determined using identical methodology.

Synthesis of Dimethylbis(phosphine)platinum(II) Complexes. Unless otherwise noted, all new complexes were prepared according to the following typical procedure. In the glovebox, a Schlenk tube equipped with a magnetic stir bar was charged with (COD)$PtMe_2$ (79.6 mg, 0.239 mmol), P(*p*-FC_6H_4)$_3$ (151.1 mg, 0.478 mmol), and either THF or CH_2Cl_2 (3−5 mL). The vessel was sealed, removed from the glovebox, and interfaced to a Schlenk line, where the mixture was stirred for ∼2 h. The volatile components were removed *in vacuo*, and the residue was triturated several times with CH_2Cl_2 (3−5 mL) to ensure complete removal of cyclooctadiene. The colorless to off-white residue was then taken up in a minimum of CH_2Cl_2. Layering with pentane afforded colorless crystals of **3i** after 1 day. Yield: 143 mg (70%). ^{1}H NMR (CD_2Cl_2): δ 0.36 (m, 6 H, Pt(CH_3)$_2$, J_{PtCH_3} = 69 Hz), 6.8−7.4 (m, 24 H, C_6H_4F). ^{31}P{^{1}H} NMR (CD_2Cl_2): δ 26.7 (s, J_{PtP} = 1888 Hz). Anal. Calcd for $C_{38}H_{30}F_6P_2Pt$: C, 53.22; H, 3.53. Found: C, 53.18; H, 3.70.

(Ph_2(pyrrolyl)P)$_2PtMe_2$ (3j) was prepared from (COD)$PtMe_2$ (72.8 mg, 0.218 mmol) and PPh_2(pyrrolyl) (109.8 mg, 0.4370 mmol). Yield: 103 mg (65%), as off-white crystals. ^{1}H NMR (CD_2Cl_2): δ 0.52 (m, 6 H, Pt(CH_3)$_2$, J_{PtCH_3} = 71 Hz), 6.25 (s, 4 H, pyrrolyl), 7.0−7.5 (m, 24 H, pyrrolyl and C_6H_5). ^{31}P{^{1}H} NMR (CD_2Cl_2): δ 69.4 (s, J_{PtP} = 2048 Hz). MS (EI) for $C_{34}H_{34}N_2P_2Pt$: calcd *m/e* 713.161 (−CH_3), 697.138 (−2CH_3), found *m/e* 713.162, 697.132.

((*p*-$CF_3C_6H_4$)$_3$P)$_2PtMe_2$ (3l) was prepared from (COD)$PtMe_2$ (62.8 mg, 0.188 mmol) and P(*p*-$CF_3C_6H_4$)$_3$ (175.1 mg, 0.376 mmol). Yield: 183 mg (84%), as irregular, transparent blocks which became opaque when dried *in vacuo*. ^{1}H NMR (CD_2Cl_2): δ 0.46 (m, 6 H, Pt(CH_3)$_2$, J_{PtCH_3} = 70 Hz), 7.4−7.7 (m, 24 H, $C_6H_4CF_3$). ^{31}P{^{1}H} NMR (CD_2Cl_2): δ 29.0 (s, J_{PtP} = 1850 Hz). Anal. Calcd for $C_{44}H_{30}F_{18}P_2Pt$: C, 45.65; H, 2.61. Found: C, 45.73; H, 2.76.

((pyrrolyl)$_3$P)$_2PtMe_2$ (3n) was prepared from (COD)$PtMe_2$ (50.6 mg, 0.152 mmol) and P(pyrrolyl)$_3$ (69.6 mg, 0.304 mmol). Yield: 63 mg (61%), as white microcrystals. ^{1}H NMR (CD_2Cl_2): δ 0.69 (m, 6 H, Pt(CH_3)$_2$, J_{PtCH_3} = 70 Hz), 6.27 (s, 6 H, pyrrolyl), 6.68 (s, 6 H, pyrrolyl). ^{31}P{^{1}H} NMR (CD_2Cl_2): δ 96.6 (s, J_{PtP} = 2506 Hz). Anal. Calcd for $C_{26}H_{30}N_6P_2Pt$: C, 45.68; H, 4.42; N, 12.29. Found: C, 45.61; H, 4.44; N, 12.15.

(Ph(pyrrolyl)$_2$P)$_2PtMe_2$ (3o) was prepared from (COD)$PtMe_2$ (49.7 mg, 0.149 mmol) and PPh(pyrrolyl)$_2$ (71.6 mg, 0.298 mmol). Yield: 82 mg (78%), as off-white microcrystals. ^{1}H NMR (CD_2Cl_2): δ 0.66 (m, 6 H, Pt(CH_3)$_2$, J_{PtCH_3} = 73 Hz), 6.25 (s, 8 H, pyrrolyl), 6.64 (m, 4H, phenyl), 6.94 (s, 8 H, pyrrolyl), 7.10 (m, 4 H, phenyl), 7.27 (m, 2 H, phenyl). ^{31}P{^{1}H} NMR (CD_2Cl_2): δ 86.5 (s, J_{PtP} = 2245 Hz). Anal. Calcd for $C_{30}H_{32}N_4P_2Pt$: C, 51.06; H, 4.57; N, 7.94. Found: C, 50.69; H, 4.44; N, 7.67.

(26) Martinho Simões, J. A.; Beauchamp, J. L. *Chem. Rev.* **1990**, *90*, 629−688.
(27) Perrin, D. D.; Armarego, W. L. F. *Purification of Laboratory Chemicals*, 3rd ed.; Pergamon: Oxford, U.K., 1988.
(28) Ojelund, G.; Wadsö, I. *Acta Chem. Scand.* **1968**, *22*, 1691−1699.
(29) Kilday, M. V. *J. Res. Natl. Bur. Stand. (U.S.)* **1980**, *85*, 467−481.
(30) Nolan, S. P.; Lopez de la Vega, R.; Hoff, C. D. *Inorg. Chem.* **1986**, *25*, 4446−4448.
(31) Nolan, S. P.; Hoff, C. D.; Landrum, J. T. *J. Organomet. Chem.* **1985**, *282*, 357−362.
(32) Costa, E.; Pringle, P. G.; Ravetz, M. *Inorg. Synth.* **1997**, *31*, 284−286.

X-ray Structural Analyses of 3b,c,n. These structures were determined from data collected on an Enraf-Nonius CAD4 diffractometer equipped with Mo Kα radiation and a low-temperature apparatus (−75 °C). Data sets were corrected for Lorentz and polarization effects and for absorption (azimuthal). The structures were solved by direct methods (MULTAN) and refined by full-matrix least-squares techniques. Atomic scattering factors, including anomalous terms for P and Pt, were taken from ref 33. In the least-squares refinement, the function minimized was $\sum w(|F_o| - |F_c|)^2$ with the weights, w, assigned as $[\sigma^2(I) + 0.0009I^2]^{-1/2}$. Crystallographic highlights are given in Table 2. Selected distances and angles are given in Table 3. Because in each complex the refinement produced some unrealistic C−H bond lengths, the hydrogen atoms were placed in idealized positions close to their previously refined positions. All non-hydrogen atoms were refined with anisotropic thermal parameters. Complete structural details, including data collection and refinement, atomic coordinates, anisotropic thermal parameters, and hydrogen atom positions, are available as Supporting Information.

X-ray Structural Analysis of 3p. The structure was determined from data collected on a Rigaku RU300 R-AXIS image plate area detector equipped with Mo Kα radiation and a low-temperature apparatus (−100 °C). The data were corrected for Lorentz and polarization effects, but not for absorption. The structure was solved by direct methods using teXsan (SIR-92) and refined by full-matrix least-squares techniques. The refinement and analysis of the structure was carried out using a package of local programs.[34] Atomic scattering factors, including anomalous terms for Cl, P, and Pt, were taken from ref 33. In the least-squares refinement, the function minimized was $\sum w(|F_o| - |F_c|)^2$ with the weights, w, assigned as $[\sigma^2(I) + 0.0009I^2]^{-1/2}$. Crystallographic highlights are given in Table 2. Selected distances and angles are given in Table 3. Because the refinement produced hydrogen thermal parameters larger than desired, the hydrogen atoms were placed in idealized positions close to their previously refined positions. All non-hydrogen atoms were refined with anisotropic thermal parameters. Two of the cyclohexyl groups (one on each phosphine ligand) are badly disordered, and no hydrogens are affixed to them. Complete structural details, including data collection and refinement, atomic coordinates, anisotropic thermal parameters, and hydrogen atom positions, are available as Supporting Information.

Acknowledgment. The National Science Foundation (Grant No. CHE-9631611) and Du Pont (Educational Aid Grant) are gratefully acknowledged for their support of this research. We also thank Prof. Matt Tarr for expert technical assistance.

Supporting Information Available: Full crystallographic details, including listings of atomic coordinates, B values, selected distances and angles, anisotropic thermal parameters, and ORTEP drawings, for complexes **3b**,**c**,**n**,**p**. This material is available free of charge via the Internet at http://pubs.acs.org.

OM9807001

(33) *International Tables for X-ray Crystallography*; Kynoch Press: Birmingham, U.K., 1974; Vol. IV.

(34) Calabrese, J. C. Central Research and Development, E. I. Du Pont de Nemours and Co., Inc., P.O. Box 80228, Wilmington, DE 19880-0228, 1991.